

Synthetic non-oxidative glycolysis enables complete carbon conservation

Igor W. Bogorad^{1,2}, Tzu-Shyang Lin¹ & James C. Liao^{1,3}

Glycolysis, or its variations, is a fundamental metabolic pathway in life that functions in almost all organisms to decompose external or intracellular sugars. The pathway involves the partial oxidation and splitting of sugars to pyruvate, which in turn is decarboxylated to produce acetyl-coenzyme A (CoA) for various biosynthetic purposes. The decarboxylation of pyruvate loses a carbon equivalent, and limits the theoretical carbon yield to only two moles of two-carbon (C₂) metabolites per mole of hexose. This native route is a major source of carbon loss in biorefining and microbial carbon metabolism. Here we design and construct a non-oxidative, cyclic pathway that allows the production of stoichiometric amounts of C₂ metabolites from hexose, pentose and triose phosphates without carbon loss. We tested this pathway, termed non-oxidative glycolysis (NOG), *in vitro* and *in vivo* in *Escherichia coli*. NOG enables complete carbon conservation in sugar catabolism to acetyl-CoA, and can be used in conjunction with CO₂ fixation¹ and other one-carbon (C₁) assimilation pathways² to achieve a 100% carbon yield to desirable fuels and chemicals.

The word glycolysis was coined in the late 1800s when researchers noticed that the concentration of glucose decreased in yeast extracts³. It was only decades later that scientists understood that native glycolytic pathways oxidize glucose to form pyruvate, which is then converted to acetyl-CoA through decarboxylation for either further oxidation or biosynthesis of cell constituents and products, including fatty acids, amino acids, isoprenoids and alcohols. Various glycolytic pathways have been discovered, including the classic Embden–Meyerhof–Parnas (EMP) pathway, the Entner–Doudoroff (ED) pathway⁴, and their variations^{5,6}, which produce acetyl-CoA from sugars through oxidative decarboxylation of pyruvate mediated by the pyruvate dehydrogenase complex or through the anaerobic pyruvate-formate lyase reaction. Similarly, the Calvin–Benson–Bassham (CBB) and ribulose monophosphate (RuMP) pathways incorporate C₁ compounds, such as CO₂ and methanol, to synthesize sugar phosphates, which then ultimately produce acetyl-CoA through pyruvate. Although the pyruvate route to acetyl-CoA, acetate⁷ and ethanol⁸ has been optimized for various purposes, the carbon loss problem has not been solved owing to inherent limitations in this pathway. Without using a CO₂ fixation pathway^{1,9,10}, the wasted CO₂ leads to a significant decrease in carbon yield. This loss of carbon has a major impact on the overall economy of biorefinery and the carbon efficiency of cell growth. On the other hand, re-fixing the lost CO₂ would incur energetic and kinetic costs.

Theoretically, it is possible to split sugars or sugar phosphates into stoichiometric amounts of acetyl-CoA in a carbon- and redox-neutral manner. Pathways without excess redox equivalents would be more efficient and could lead to maximal yields¹¹. However, no such pathway is known to exist. Here we constructed the cyclic NOG pathway (Fig. 1a) to break down sugars or sugar phosphates into the theoretical maximum amount of C₂ metabolites without carbon loss.

The metabolic logic of the cyclic NOG pathway can be understood by breaking it down into three sections (Fig. 1a). First, fructose 6-phosphate (F6P) is the input molecule, and the pathway requires

an additional investment of two F6P molecules. Second, the three F6P molecules are broken down to three acetyl phosphate (AcP) and three erythrose 4-phosphate (E4P) molecules by the phosphoketolases. This irreversible step provides the first driving force for NOG. Third, these three E4P molecules then undergo carbon rearrangement to regenerate the two initially invested F6P molecules (Fig. 1b). The net reaction results in the irreversible formation of three AcP molecules. Phosphoketolases are known to have either F6P activity (termed Fpk) or xylulose 5-phosphate (X5P) activity (termed Xpk). Even though the product of Xpk is different from Fpk (glyceraldehyde 3-phosphate (G3P) is formed, as opposed to E4P), both are metabolically equivalent when Xpk is used in combination with transketolase (Tkt) (Supplementary Fig. 1a).

The regeneration of two F6P from three E4P can occur in several different ways. Figure 1b shows a fructose 1,6-bisphosphate (FBP)-dependent network, and Supplementary Fig. 1b shows a sedoheptulose 1,7-bisphosphate (SBP)-dependent network, with carbon rearrangement schemes illustrated by the colour-coded carbon atoms. The FBP-dependent network involves transaldolase (Tal), FBP aldolase (Fba) and fructose 1,6-bisphosphatase (Fbp). The SBP-dependent network does not involve Tal, but requires SBP aldolase and sedoheptulose 1,7-bisphosphatase. The two bisphosphatases provide the second irreversible driving force to ensure that carbon rearrangement proceeds towards the formation of F6P. Analogous systems of carbon rearrangement¹² are used in several natural pathways, such as the CBB, RuMP and the pentose phosphate pathways (see Supplementary Fig. 2).

Because there are two different possible phosphoketolase activities (Fpk and Xpk, shown in Supplementary Fig. 1a) and two variations of the carbon rearrangement networks (Supplementary Fig. 1bc), many combinations can be devised. For each of the carbon rearrangement networks, three configurations exist that form a basis^{13,14} to all other combinations (Fig. 2a–c): (1) NOG using only Fpk; (2) NOG using only Xpk; and (3) NOG using one Fpk with two Xpk activities but without the use of one type of Tkt reaction—the reversible conversion of F6P and G3P to E4P and ribose 5-phosphate (R5P). Figure 2a–c shows the three modes of NOG using the FBP-dependent carbon rearrangement network. In these configurations, the carbon rearrangement network and the phosphoketolase system are integrated such that the pathways appear different from those shown in Fig. 1b. Similarly, three modes of NOG can be derived for the SBP-dependent carbon rearrangement network. Combinations of these modes can generate infinite numbers of variations for NOG. NOG can be used in combination with other pathways, such as the CBB and RuMP pathways, which produce F6P from C₁ compounds (Fig. 1a). In addition, NOG can also use pentose or triose sugar phosphates as input (Supplementary Fig. 3).

To validate the feasibility of this pathway experimentally, we constructed systems to demonstrate NOG both *in vitro* and *in vivo*. To construct an *in vitro* system, we cloned a putative phosphoketolase which has both Fpk and Xpk activities (F/Xpk) from *Bifidobacterium adolescentis* and Tal, Tkt, Fbp, ribulose-5-phosphate epimerase (Rpe),

¹Department of Chemical and Biomolecular Engineering, University of California, Los Angeles, 420 Westwood Plaza, Los Angeles, California 90095, USA. ²Department of Bioengineering, University of California, Los Angeles, 420 Westwood Plaza, Los Angeles, California 90095, USA. ³Institute for Genomics and Proteomics, University of California, Los Angeles, 420 Westwood Plaza, Los Angeles, California 90095, USA.

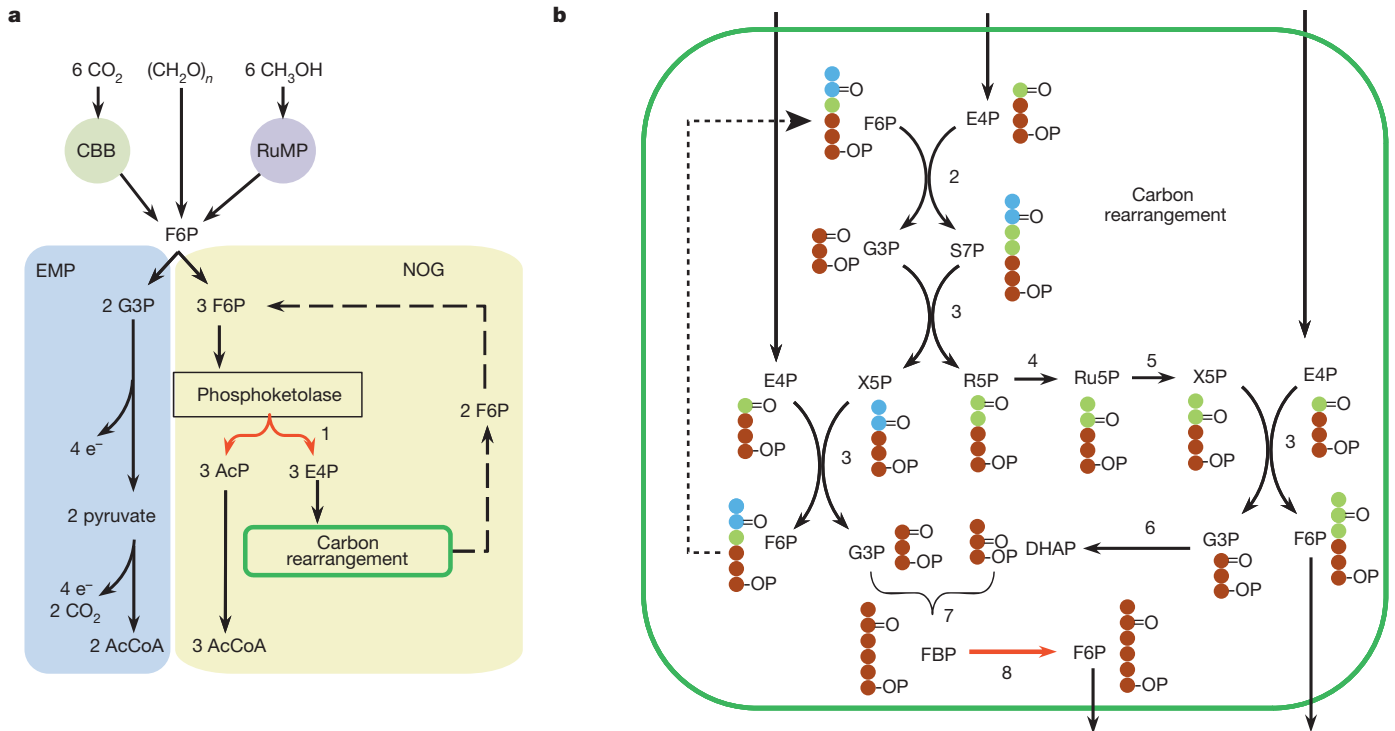


Figure 1 | Structure of oxidative (EMP) and non-oxidative glycolysis (NOG). **a**, Simplified schematic of EMP and NOG. **b**, An example of the carbon rearrangement network involving FBP. The red arrow indicates the irreversible phosphoketolase reaction. The carbon colour scheme illustrates

ribose-5-phosphate isomerase (Rpi) and acetate kinase (Ack) from *E. coli* with a His tag (Supplementary Figs 4 and 5) for one-step purification. Other enzymes, namely Fba, triose phosphate isomerase (Tpi), glycerol-3-phosphate dehydrogenase (Gpd), hexokinase (Glk), glucose-6-phosphate dehydrogenase (Zwf), phosphoglucose isomerase (Pgi) and phosphofructokinase (Pfk) were purchased. The His-tag enzymes were tested for activity (Supplementary Fig. 6 and Supplementary Table 1) and mixed together in a properly selected reaction buffer. This core system (F/Xpk, Tal, Tkt, Rpe, Rpi, Tpi, Fba, Fbp) was ATP and redox independent and consisted of eight core enzymes which convert one F6P molecule to three AcP molecules. The initial 10 mM F6P was completely converted to stoichiometric amounts of AcP (within error) at room temperature (25 °C) after 1.5 h (Fig. 3a). To extend the production

carbon rearrangement. Hydroxyl groups are not shown. Enzyme numbers are indicated: 1, phosphoketolase; 2, Tal; 3, Tkt; 4, Rpi; 5, Rpe; 6, Tpi; 7, Fba; 8, Fbp. DHAP, dihydroxyacetone phosphate; Ru5P, ribulose 5-phosphate.

further to acetate, Ack, phosphofructokinase (Pfk) and ADP were added to the *in vitro* NOG system. By adding a futile ATP-burning cycle^{15,16} using Pfk and Fbp, the complete conversion to acetate was possible (Fig. 3b). Similar *in vitro* NOG systems were tested on R5P and G3P, which produced nearly theoretical amounts of AcP at a ratio of 2.3 and 1.6, respectively (Fig. 3c). These *in vitro* results demonstrated the feasibility of NOG and paved the way for *in vivo* testing.

Next, NOG was engineered into the model organism *E. coli*. Xylose, instead of glucose, was used because it is the second most abundant sugar on Earth, and it avoids the use of the phosphotransferase system (PTS) for transport¹⁷, which is phosphoenolpyruvate (PEP) dependent and is associated with complex regulatory mechanisms¹⁸. To engineer NOG for xylose in *E. coli*, it was necessary to overexpress two enzymes:

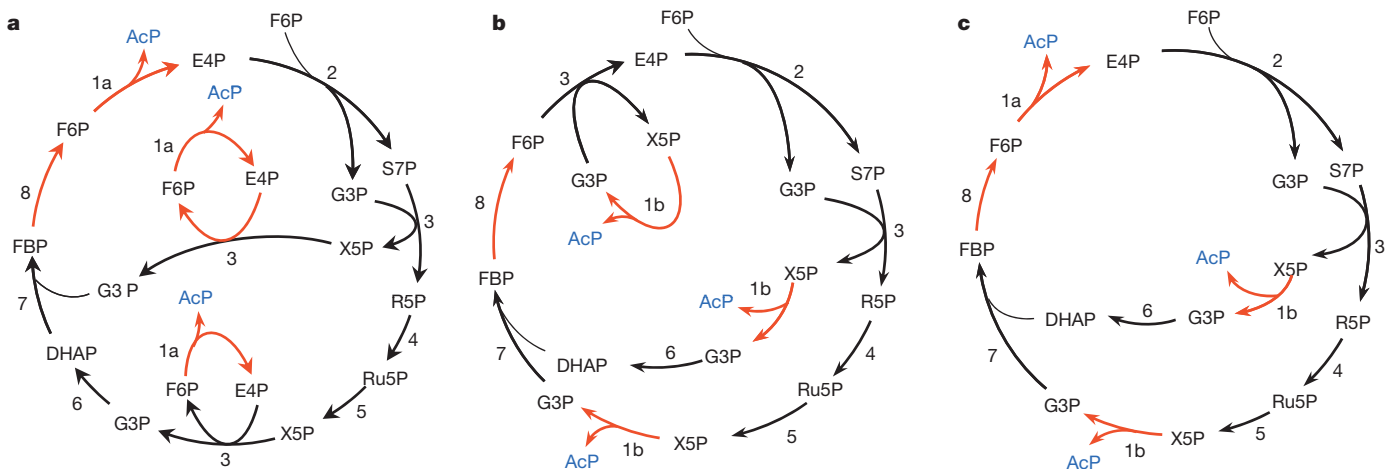


Figure 2 | Three FBP-dependent NOG networks. **a–c**, NOG using Fpk only (**a**), NOG using Xpk only (**b**) and NOG using F/Xpk (**c**). These configurations differ from those shown in Fig. 1 because the Xpk-linked Tkt has been

integrated with carbon rearrangement. The red arrows in **a–c** indicate irreversible reactions that drive the cycle. Enzyme numbers are defined in Fig. 1 legend, except: 1a, Fpk; 1b, Xpk.

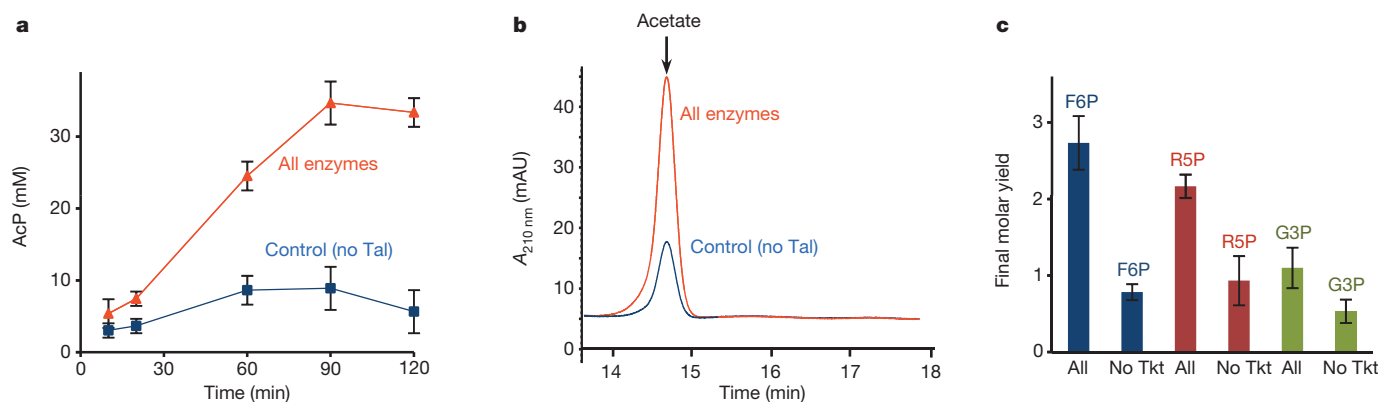


Figure 3 | In vitro NOG. **a**, *In vitro* conversion of F6P to AcP using eight purified core enzymes, including F/Xpk, Fbp, Fba, Tkt, Tal, Rpi, Rpe and Tpi. The starting F6P concentration was 10 mM. The red triangles are reactions with all eight enzymes present. The blue squares are reactions with all enzymes except Tal. **b**, *In vitro* conversion of F6P to acetate, determined by HPLC. The addition of Ack and Pfk allowed the complete conversion of AcP to acetate.

Acetate was monitored at 210 nm ($A_{210\text{nm}}$). **c**, Conversion of three sugar phosphates—F6P, R5P and G3P—to near stoichiometric amounts of AcP. 10 mM of each substrate was converted to AcP using the same core enzymes (denoted ‘all’), whereas ‘no Tkt’ controls produced much less. *In vitro* enzyme assays were independently performed in triplicates and error bars indicate standard deviation (s.d.).

F/Xpk (encoded by *fxpk* from *B. adolescentis*) and Fbp (encoded by *E. coli fbp*). Other enzymes in NOG were natively expressed in *E. coli* under experimental conditions. The genes encoding F/Xpk and Fbp were cloned on a high-copy plasmid (pIB4) under the control of the P_{lacO_1} (ref. 19) isopropylthiogalactoside (IPTG)-inducible promoter. The plasmid was transformed into three *E. coli* strains: JCL16 (wild type), JCL166 (ref. 20) ($\Delta ldhA \Delta adhE \Delta frdBC$) and JCL118 ($\Delta ldhA \Delta adhE \Delta frdBC \Delta pflB$). The latter two strains were used to avoid fermentative pathways that compete with NOG for F6P utilization (Fig. 4a). High-pressure liquid chromatography (HPLC) was used for monitoring xylose consumption and organic acid formation.

The dual expression of F/Xpk and Fbp in JCL188 was demonstrated by protein electrophoresis (Supplementary Fig. 5) and their activities were confirmed by a colorimetric enzyme assay (Fig. 4b). After an initial aerobic growth phase for cell growth and protein induction, high-cell-density cells were harvested and re-suspended in anaerobic minimal medium with xylose at a final optical density ($OD_{600\text{nm}}$) of 9. Anaerobic conditions were used to avoid the oxidation of acetate through the tricarboxylic acid (TCA) cycle. The wild-type host (JCL16) with plasmid pIB4 produced a mixture of lactate, formate, succinate and acetate from xylose, and the yield of acetate was quite low at about 0.4 acetates produced per xylose consumed. By introducing $\Delta ldhA$, $\Delta adhE$ and $\Delta frdBC$ knockouts (JCL166), and with plasmid pIB4, the yield was increased to 1.1 acetates per xylose (5.1 g l^{-1} in 16 h) consumed. After further deleting *pflB* (JCL118) and adding pIB4, the titre reached a maximum of only 3.6 g l^{-1} in 16 h. However, the yield reached the highest level of 2.2 acetates per xylose consumed, approaching the theoretical maximum of 2.5 moles of acetate per mole of xylose (Fig. 4c), and exceeding the theoretical maximum of 1.67 moles of acetate per mole of xylose supported by the EMP pathway only. Even though the rate of acetate production decreased, which is a complex result of enzymatic kinetics and regulation, the increase in yield supported the *in vivo* activity of NOG. Some succinate remained, presumably due to succinate dehydrogenase (*sdhABCD*) left over from the aerobic growth phase. These results indicate that NOG is also feasible *in vivo*. With further optimization, NOG represents a practical alternative for acetyl-CoA biosynthesis in various applications.

When NOG is used to degrade glucose, the net reaction is two ATP and three acetate molecules per glucose, while no reducing equivalents are generated. Therefore, NOG may not be important for normal cellular growth, which requires reducing equivalents and metabolites in the EMP pathway. These features may explain why NOG has not been found in nature. The challenges for re-routing glycolysis to NOG

in *E. coli* for growth involve (1) replacing the PTS-glucose transport system with a system that does not depend on PEP, (2) deleting the lower part of the EMP pathway, (3) adapting the *E. coli* strain to grow under this newly wired central metabolism, and (4) providing alternative source of reducing power. ^{13}C -labelled substrate can be used to determine the relative flux of each pathway based on the rearrangement pattern depicted in Fig. 1b. When a sugar (such as xylose or glucose) is used as the initial substrate to generate the input to NOG, acetate can be produced without carbon loss and without additional input of reducing equivalents. Once additional reducing power is provided in the form of hydrogen or formic acid²¹, NOG can be used to produce compounds that are more reduced than acetate, such as ethanol, 1-butanol, isoprenoids and fatty acids²².

The critical enzyme in NOG is F/Xpk, which is used in nature in the heterofermentative phosphoketolase pathway (PKP) and in the bifid shunt (Supplementary Fig. 7). PKP has a relatively low net ATP yield of one ATP per glucose consumed (Supplementary Table 2). Xpk has also been found in many organisms, such as *Clostridium acetobutylicum*, in which up to 40% of xylose is degraded by the PKP²³. *Bifidobacteria* utilize the unique bifid shunt²⁴ (Supplementary Fig. 7d), which oxidizes two glucoses into two lactates and three acetates. This fermentative pathway increases the ATP yield to 2.5 ATP per glucose, compared with 2 ATP per glucose for lactate fermentation through the EMP (Supplementary Table 2). In both phosphoketolase variants (PKP and the bifid shunt), G3P continues through the oxidative part of the EMP pathway to form pyruvate. Thus they are not able to directly convert glucose to three two-carbon compounds.

Acetogens, such as *Moorella thermoacetica*²⁵, achieve carbon conservation by fixing CO_2 emitted from pyruvate via the Wood–Ljungdahl pathway (Supplementary Fig. 7e). However, this pathway contains complex enzymes to overcome significant kinetic or thermodynamic barriers²⁶. By contrast, NOG contains no difficult enzymes and is amenable to heterologous expression (Supplementary Tables 3–5 and Supplementary Fig. 8). NOG can also be used in conjunction with C1 assimilation pathways that synthesize acetyl-CoA via pyruvate. When combined with the CBB cycle, NOG provides complete carbon conversion in the synthesis of acetyl-CoA from CBB intermediates such as F6P or G3P. NOG coupled with the CBB pathway requires less ATP to synthesize one molecule of acetyl-CoA. Perhaps more importantly than saving ATP is that NOG requires less turnover of Rubisco for acetyl-CoA synthesis (Supplementary Table 6). For each acetyl-CoA produced, only two CO_2 molecules need to be fixed by Rubisco, as opposed to three CO_2 in the case of the CBB–EMP pathway combination with pyruvate dehydrogenase. This improved efficiency would become

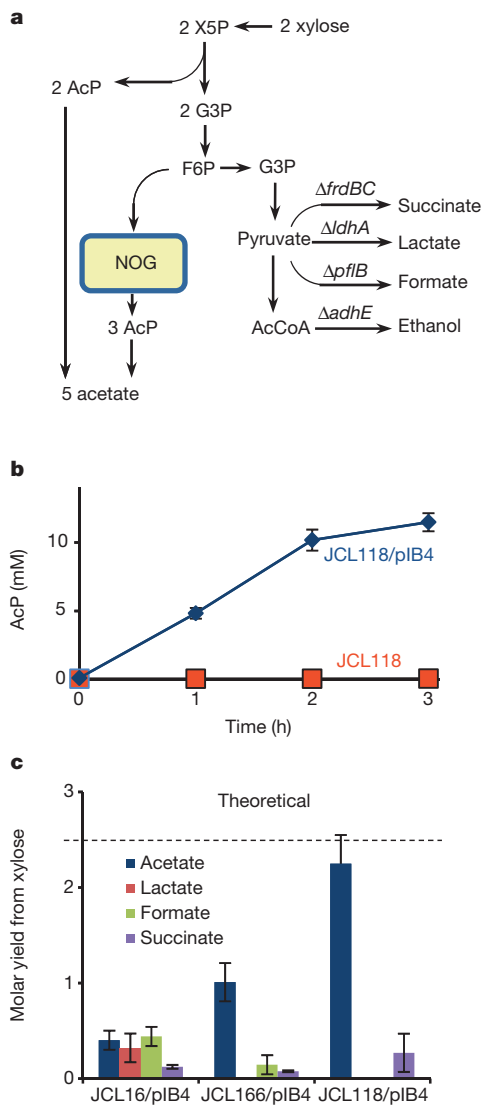


Figure 4 | *In vivo* conversion of xylose to acetate using NOG. **a**, Pathways in *E. coli* strains (JCL16, JCL166, JCL118) with NOG for converting xylose to acetate and other competing products (lactate, ethanol, succinate and formate production). Plasmid pIB4 was transformed into these strains for the expression of F/Xpk (from *B. adolescentis*) and Fbp (from *E. coli*) under the control of the $P_{l\text{lac}O_1}$ promoter. **b**, The expression of Fbp and F/Xpk in JCL118/pIB4 was tested by purifying the crude extract on a His-tag column, and then running a coupled colorimetric assay to test AcP formation. The control was JCL118 (without plasmid), which did not produce AcP. **c**, Xylose was converted to acetate and other products under anaerobic conditions. Strain JCL118 ($\Delta\text{ldhA}\Delta\text{adhE}\Delta\text{frdBC}\Delta\text{pf1B}$) produced a near theoretical ratio of acetate/xylose. *In vivo* production data were independently repeated three separate times from frozen glycerol stocks. Error bars indicate s.d.

especially important if an autotrophic organism was used for the biosynthesis of acetyl-CoA-derived products, such as 1-butanol²⁷ or fatty acids²⁸. Using NOG with the CBB pathway would represent a 50% increase in carbon efficiency in acetyl-CoA biosynthesis over native pathways. In view of the relatively low turnover number of Rubisco²⁹, this increased efficiency could allow faster production of acetyl-CoA-derived compounds. Given the variety of possible applications, NOG seems to be fundamentally important for carbon management.

METHODS SUMMARY

All NOG enzymes were constructed with amino-terminal His tags using the pQE9 from Qiagen. The genomic template for the *E. coli* genes was JCL16. JCL16 is wild-type *E. coli* strain BW25113 with F' transduced from XL-1 (Tet^R). JCL166 is JCL16 but with ΔldhA , ΔadhE and ΔfrdBC . JCL118 is similar

to JCL166 but with Δpf1B . The genomic template for F/Xpk was from *B. adolescentis* ATCC 15703. Many coupled enzyme assays measured the activity of the enzymes by measuring AcP at 505 nm or NAD(P)H at 340 nm. Plasmid pIB4 was constructed using the pZE12 (ref. 19) backbone with His-tagged Fbp and F/Xpk under the $P_{l\text{lac}O_1}$ promoter and was transformed into all production strains. For *in vivo* production, strains were grown aerobically on Luria–Bertani (LB) broth with 5% xylose, induced with 0.1 mM IPTG for 5 h, concentrated, and resuspended in fresh M9 5% xylose media. Organic acid and sugar concentration were monitored by HPLC using the HPX-87H column.

Online Content Any additional Methods, Extended Data display items and Source Data are available in the online version of the paper; references unique to these sections appear only in the online paper.

Received 5 February; accepted 15 August 2013.

Published online 29 September; corrected online 30 September and 30 October 2013 (see full-text HTML version for details).

- Bassham, J. *et al.* The path of carbon in photosynthesis. XXI. The cyclic regeneration of carbon dioxide acceptor. *J. Am. Chem. Soc.* **76**, 1760–1770 (1954).
- Yurimoto, H., Kato, N. & Sakai, Y. Assimilation, dissimilation, and detoxification of formaldehyde, a central metabolic intermediate of methylotrophic metabolism. *Chem. Rec.* **5**, 367–375 (2005).
- Nelson, D. & Cox, M. *Lehninger Principles of Biochemistry* (W. H. Freeman, 2005).
- Peekhaus, N. & Conway, T. What's for dinner?: Entner-Doudoroff metabolism in *Escherichia coli*. *J. Bacteriol.* **180**, 3495–3502 (1998).
- Gutler, J.-K. *et al.* Cell-free metabolic engineering: production of chemicals by minimized reaction cascades. *ChemSusChem* **5**, 2165–2172 (2012).
- Ye, X. *et al.* Synthetic metabolic engineering—a novel, simple technology for designing a chimeric metabolic pathway. *Microb. Cell Fact.* **11**, 120 (2012).
- Causey, T. & Ingram, L. Engineering the metabolism of *Escherichia coli* W3110 for the conversion of sugar to redox-neutral and oxidized products: homoacetate production. *Proc. Natl Acad. Sci. USA* **100**, 825–832 (2003).
- Tao, H., Gonzalez, R., Martinez, A. & Ingram, L. Engineering a homo-ethanol pathway in *Escherichia coli*: increased glycolytic flux and levels of expression of glycolytic genes during xylose fermentation. *J. Bacteriol.* **183**, 2979–2988 (2001).
- Berg, I. A., Kockelkorn, D., Buckel, W. & Fuchs, G. A 3-hydroxypropionate/4-hydroxybutyrate autotrophic carbon dioxide assimilation pathway in Archaea. *Science* **318**, 1782–1786 (2007).
- Ragsdale, S. W. & Pierce, E. Acetogenesis and the Wood–Ljungdahl pathway of CO₂ fixation. *Biochim. Biophys. Acta* **1784**, 1873–1898 (2008).
- Dugar, D. & Stephanopoulos, G. Relative potential of biosynthetic pathways for biofuels and bio-based products. *Nature Biotechnol.* **29**, 1074–1078 (2011).
- Meléndez-Hevia, E. & Isidoro, A. The game of the pentose phosphate cycle. *J. Theor. Biol.* **117**, 251–263 (1985).
- Liao, J. C., Hou, S.-Y. & Chao, Y.-P. Pathway analysis, engineering, and physiological considerations for redirecting central metabolism. *Biotechnol. Bioeng.* **52**, 129–140 (1996).
- Schuster, R. & Schuster, S. Refined algorithm and computer program for calculating all non-negative fluxes admissible in steady states of biochemical reaction systems with or without some flux. *Comput. Appl. Biosci.* **9**, 79–85 (1993).
- Daldal, F. & Fraenkel, D. Assessment of a futile cycle involving reconversion of fructose 6-phosphate to fructose 1, 6-bisphosphate during gluconeogenic growth of *Escherichia coli*. *J. Bacteriol.* **153**, 390–394 (1983).
- Patnaik, R., Roof, W. D., Young, R. F. & Liao, J. C. Stimulation of glucose catabolism in *Escherichia coli* by a potential futile cycle. *J. Bacteriol.* **174**, 7527–7532 (1992).
- Roseman, S. & Meadow, N. D. Signal transduction by the bacterial phosphotransferase system. *J. Biol. Chem.* **265**, 2993–2996 (1990).
- Gonzalez, R., Tao, H., Shanmugam, K. T., York, S. W. & Ingram, L. O. Global gene expression differences associated with changes in glycolytic flux and growth rate in *Escherichia coli* during the fermentation of glucose and xylose. *Biotechnol. Prog.* **18**, 6–20 (2002).
- Lutz, R. & Bujard, H. Independent and tight regulation of transcriptional units in *Escherichia coli* via the LacR/O, the TetR/O and AraC/I₁–I₂ regulatory elements. *Nucleic Acids Res.* **25**, 1203 (1997).
- Atsumi, S. *et al.* Metabolic engineering of *Escherichia coli* for 1-butanol production. *Metab. Eng.* **10**, 305–311 (2008).
- Li, H. *et al.* Integrated electromicrobial conversion of CO₂ to higher alcohols. *Science* **335**, 1596 (2012).
- Gronenberg, L. S., Marcheschi, R. J. & Liao, J. C. Next generation biofuel engineering in prokaryotes. *Curr. Opin. Chem. Biol.* **17**, 462–471 (2013).
- Liu, L. *et al.* Phosphoketolase pathway for xylose catabolism in *Clostridium acetobutylicum* revealed by ¹³C-metabolic flux analysis. *J. Bacteriol.* **194**, 5413–5422 (2012).
- Yin, X., Chambers, J. R., Barlow, K., Park, A. S. & Wheatcroft, R. The gene encoding xylulose-5-phosphate/fructose-6-phosphate phosphoketolase (*xfp*) is conserved among *Bifidobacterium* species within a more variable region of the genome and both are useful for strain identification. *FEMS Microbiol. Lett.* **246**, 251–257 (2005).
- Drake, H. L. & Daniel, S. L. Physiology of the thermophilic acetogen *Moorella thermoacetica*. *Res. Microbiol.* **155**, 869–883 (2004).
- Ragsdale, S. W. Metals and their scaffolds to promote difficult enzymatic reactions. *Chem. Rev.* **106**, 3317–3337 (2006).
- Lan, E. I. & Liao, J. C. ATP drives direct photosynthetic production of 1-butanol in cyanobacteria. *Proc. Natl Acad. Sci. USA* **109**, 6018–6023 (2012).

28. Liu, X., Sheng, J. & Curtiss, R. Fatty acid production in genetically modified cyanobacteria. *Proc. Natl Acad. Sci. USA* **108**, 6899–6904 (2011).
29. Tcherkez, G. G. B., Farquhar, G. D. & Andrews, T. J. Despite slow catalysis and confused substrate specificity, all ribulose biphosphate carboxylases may be nearly perfectly optimized. *Proc. Natl Acad. Sci. USA* **103**, 7246–7251 (2006).

Supplementary Information is available in the online version of the paper.

Acknowledgements This work was partially supported by National Science Foundation (NSF) grant MCB-1139318 and Department of Energy (DOE) grant

DEO-SC0006698. I.W.B. was supported by NSF Integrative Graduate Education and Research Traineeship (IGERT) grant no. 0903720.

Author Contributions I.W.B. and J.C.L. conceived the project, designed the experiments, analysed the data, and wrote the manuscript. I.W.B. performed experiments, and T.-S.L. assisted in experiments.

Author Information Reprints and permissions information is available at www.nature.com/reprints. The authors declare no competing financial interests. Readers are welcome to comment on the online version of the paper. Correspondence and requests for materials should be addressed to J.C.L. (ljiao@ucla.edu).

METHODS

Culture media, chemicals, and conditions. *E. coli* cultures were grown in Luria-Bertani (LB) broth with appropriate antibiotics at 37 °C at 250 r.p.m. Antibiotics were added at the following concentrations: ampicillin, 100 µg ml⁻¹; and kanamycin, 50 µg ml⁻¹. All chemicals and substrates were purchased from Sigma-Aldrich unless otherwise indicated.

Plasmid construction. Plasmids for expressing N-terminal polyhexahistidine-tagged Tkt, Tal, Rpe, Rpi, Ack, Fbp and F/Xpk were constructed using a modification of the ligation-independent cloning (LIC)³⁰ method using pQE9 (Qiagen) as the vector backbone. The primers used are listed in Supplementary Table 6. The genomic template for the *E. coli* genes was JCL16 (BW25113 strain). The genomic template for F/Xpk was from *B. adolescentis* ATCC 15703. Plasmid pIB4 was constructed using pZE12 (ref. 19) as the vector backbone with His-tagged Fbp and F/Xpk under the control of the same P₁lacO₁ promoter.

Protein purification. All in-house His-tagged proteins were purified by affinity chromatography using His-Spin Protein Miniprep kit (Zymo Research). Protein concentration was measured using diluted samples with Coomassie Plus Assay Reagent (Pierce) and bovine serum albumin (Bio-Rad) as the standard curve.

Enzyme assays. All enzymes were assayed using the same enzyme buffer, consisting of 50 mM Tris pH 7.5, 5 mM MgCl₂, 5 mM potassium phosphate. Cofactors were added where needed. The enzymes Fba, Glk, Zwf, Tpi and Gpd were purchased from Sigma-Aldrich. Each individual enzyme assay is described later and the reaction schemes are illustrated in Supplementary Fig. 6. All substrates were purchased from Sigma-Aldrich.

Assay for Ack. Ack was measured using both enzyme-linked assay and colorimetric hydroxamate assay for AcP consumption. The enzyme-linked assay coupled ATP formation with the formation of NADPH with a molar extinction coefficient at 340 nm (ϵ_{340} equal to 6.2 mM⁻¹ cm⁻¹) using commercial Glk and Zwf. This assay included the addition of 1 mM ADP, 2 mM glucose, 0.2 mM NADP, 0.5 U Glk, 0.5 U Zwf and 5 mM AcP. The activities of the linked enzymes were not limiting. In the colorimetric assay, AcP is reacted to form the brown ferric acetyl-hydroxamate measured at 505 nm. This end-point assay was stopped by adding 40 µl of assay solution to 60 µl of 2 M hydroxylamine pH 6.5. After 10 min, the colouring reagent consisting of 40 µl of 15% trichloroacetic acid, 40 µl of 4 M HCl, and 40 µl of FeCl₃ in 0.1 M HCl was added. A standard curve using commercial lithium potassium AcP was used to relate absorbance to concentration, which showed a linear relationship between 0 to 15 mM in the conditions described. Thus, the hydroxamate method was also used to directly measure the consumption of AcP by Ack.

Assay for F/Xpk. F/Xpk activity was also assayed using both the enzyme-linked ultraviolet assay and the end-point colorimetric assay. For the ultraviolet method,

the assay was similar to Ack except for the addition of 1 mM of thiamine pyrophosphate (TPP), 2.5 µg of purified F/Xpk, and 10 mM of substrate. Fpk activity was measured using F6P as the substrate. To measure Xpk activity, the addition of more than 2 U of Rpe and Rpi each allowed the use of R5P as the substrate (X5P was not available). The hydroxamate method was also used to directly measure the production of AcP from F6P or R5P.

Assay for Tkt. His-tagged Tkt was assayed using an enzyme-linked system to NADH (ϵ_{340} = 6.2 mM⁻¹ cm⁻¹) consumption with Tpi and Gpd. Because X5P was unavailable commercially, excess Rpi and Rpe were added in order to use R5P as the initial substrate. 1 mM TPP, 0.2 mM NADH, 5 mM R5P and over 2 U Tpi, 0.5 U Gpd, over 2 U Rpe and over 2 U Rpi was added to the enzyme buffer.

Assay for Tal. Tal was assayed in the reverse direction and coupled to NADPH production by Zwf. 2 U Rpe, over 2 U Rpi, 5 mM R5P, 95 µg Tkt, 1.2 µg Tal, over 2 U Pgi and 0.5 U Zwf was added to the enzyme buffer.

Assay for Fbp. Fbp was also assayed by NADPH production. Over 2 U Pgi, 1 µg Fbp and 0.5 U Zwf was added to the enzyme buffer.

In vitro NOG to convert F6P, R5P, G3P to AcP. 10 mM of each substrate was used as a substrate in enzyme buffer with 1 mM TPP with an additional 50 mM potassium phosphate. The following eight purified enzymes were included in the reaction mix: 0.1 U F/Xpk, 0.5 U Tkt, 0.5 U Tal, over 2 U Tpi, over 2 U Rpe, over 2 U Rpi, 0.2 U Fbp and 0.5 U Fba. AcP concentration (by hydroxamate assay) was measured over 2 h.

Construction of in vivo NOG strains. JCL16 is BW25113 with F' transduced from XL-1 (Tet^R). JCL166 is JCL16 but with Δ ldhA, Δ adhE and Δ frdBC. JCL118 is the same as JCL166 but with Δ pfkB. Gene knockouts were made using respective donor strains from the Keio collection³¹ using P1 transduction.

In vivo NOG production from xylose. These strains were transformed with pIB4 and grown initially aerobically in LB broth with 5% xylose. At semi-log phase the cultures were induced for 5 h using 0.1 mM IPTG. The cells were then harvested, concentrated, and re-suspended anaerobically at an optical density (OD_{600 nm}) of 9 in minimal M9 media with 5% xylose. Products from xylose from JCL16 were compared to JCL166 and JCL118 with pIB4 and analysed by an Agilent 1200 HPLC. Organic acids (succinate, lactate, formate and acetate) were detected at 210 nm by the Aminex HPX-87H (Bio-Rad) column using isocratic 5 mM sulphuric acid as the mobile phase at 0.6 ml min⁻¹ flow rate with 20 µl injection volume at 30 °C column temperature. The refractive index detector was used to measure the concentration of xylose.

30. Aslanidis, C. & de Jong, P. J. Ligation-independent cloning of PCR products (LIC-PCR). *Nucleic Acids Res.* **18**, 6069–6074 (1990).
31. Baba, T. *et al.* Construction of *Escherichia coli* K-12 in-frame, single-gene knockout mutants: the Keio collection. *Mol. Syst. Biol.* **2**, 2006.0008 (2006).